J. Biochem. 2010;148(1):47–54 doi:10.1093/jb/mvq032

JB THE JOURNAL OF BIOCHEMISTRY

Stopped flow kinetic studies on reductive half-reaction of histamine dehydrogenase from *Nocardioides simplex* with histamine

Received February 22, 2010; accepted March 13, 2010; published online March 19, 2010

Maiko Tsutsumi, Seiya Tsujimura, Osamu Shirai and Kenji Kano*

Division of Applied Life Sciences, Graduate School of Agriculture, Kyoto University, Sakyo-ku, Kyoto 606-8502, Japan

*Kenji Kano, Division of Applied Life Sciences, Graduate School of Agriculture, Kyoto University, Sakyo-ku, Kyoto 606-8502, Japan
Tel: +81 75 753 6392, Fax: +81 75 753 6456,
email: kkano@kais.kyoto-u.ac.jp

Histamine dehydrogenase from *Nocardioides simplex* (HmDH) which catalyzes the oxidative deamination of histamine is an iron–sulphur–containing flavoprotein. For our further understanding on the intramolecular electron transfer process, the reductive half reaction of HmDH with histamine has been studied by stopped flow spectrophotometry at pH 7.5 and 10. The reaction at pH 7.5 is found to be analysed on a kinetic model composed of three sequential first-order reactions. The first fast phase, of which the rate constant shows a hyperbolic dependence on the histamine concentration, is assigned to a direct two-electron reduction of the oxidized flavin ($CFMN_O$) by histamine with no involvement of the semiquinone form of the flavin ($CFMN_S$). The second moderate process is the substrate-independent intramolecular single-electron transfer from the reduced flavin to the oxidized iron–sulphur cluster. The third slow process is considered to reflect the second binding of histamine to $CFMN_S$, which is responsible for the substrate inhibition. At pH 10, the reaction is analysed with one pseudo-first-order reaction phase which is substrate-dependent two-electron reduction of $CFMN_O$ coupled with the subsequent fast intersubunit single-electron transfer. The UV–vis spectroscopy of HmDH suggests the deprotonation of Tyr residues, which seems to cause the switching of the electron transfer property.

Keywords: Histamine dehydrogenase/6-*S*-cysteinyl flavin mononucleotide/[4Fe-4S] iron-sulphur cluster/intramolecular electron transfer/substrate inhibition.

Abbreviations: HmDH, histamine dehydrogenase from *Nocardioides simplex*; CFMN, 6-*S*-cysteinyl flavin mononucleotide; TMADH, trimethylamine dehydrogenase from *Methylophilis methyrotrophic* sp. W3A1; $CFMN_O$, the oxidized form of CFMN; $CFMN_S$, the semiquinone form of CFMN; $CFMN_R$, the fully reduced form of CFMN; FeS_O, the oxidized form of [4Fe-4S] iron–sulphur cluster; FeS_R, the reduced form of [4Fe-4S] iron–sulphur cluster.

The iron–sulphur flavoprotein histamine dehydrogenase isolated from *Nocardioides simplex* (HmDH) catalyzes the oxidative deamination of histamine to imidazole acetaldehyde and ammonia. HmDH is an enzyme which contains two redox centers and a homodimer of 76 kDa molecular mass subunits. Each subunit contains a covalently bound 6-*S*-cysteinyl FMN (CFMN) and a [4Fe-4S] iron–sulphur cluster (FeS), as well as one equivalent of tightly bound adenosine diphosphate with unknown function (*1*, *2*). The DNA sequence alignment shows that HmDH is closely related to histamine dehydrogenase from *Rhizobium* sp. 4–9 (64% identical) and trimethylamine dehydrogenase from *Methylophilis methyrotrophic* sp. W3A1 (TMADH, 40% identical), both of which also contain one CFMN and one FeS per subunit (*1*, *2*). These iron–sulphur-containing flavoproteins require three electrons per subunit for full reduction; two for the full reduction of the flavin and one for the reduction of iron–sulphur cluster. It has been considered that in HmDH two electrons in the substrate are passed to the oxidized CFMN ($CFMN_O$) and two sequential single-electron transfers occur from the fully reduced CFMN ($CFMN_R$) to the oxidized FeS (FeS_O) and finally another two sequential single-electron transfers are followed from the reduced FeS (FeS_R) to an electron acceptor (*3*, *4*).

The unique redox properties of HmDH are observed in the reductive titration with dithionite and histamine. The enzyme is completely reduced with dithionite to generate a three-electron reduced subunit. In contrast, in the reductive titration with histamine, a two-electron reduction occurs per subunit of the enzyme at pH <9, but the switching occurs in the electron transfer property at around pH 9: a single-electron reduction proceeds per subunit at pH >9 (*3*). The titration experiments have also allowed absorption spectral assignment of the semiquinone form of CFMN ($CFMN_S$) and $CFMN_R$. The enzyme reduced with one molecule of histamine per subunit corresponds to the enzyme composed of the two-electron-reduced subunits. The two-electron-reduced form of HmDH subunit is in equilibrium between two ultimate states: one involves $CFMN_S$ and FeS_R ($CFMN_S$-FeS_R state) and the other involves $CFMN_R$ and FeS_O ($CFMN_R$-FeS_O state) (*3*). The distribution is controlled by individual redox potentials which are functions of pH (*3*). At pH >9, HmDH is reduced to generate a homodimer composed of the single-electron-reduced subunit ($CFMN_S$–FeS_O state subunit) (*3*). These unique redox properties can be explained in term of the redox potential of the cofactors (*3*). However, the

redox kinetics and the factors to cause the switching in the redox property remain to be elucidated.

We have also cloned the *hmd* gene and overexpressed HmDH (*1*) and several site-directed mutants in *Escherichia coli* (*4*). The thermodynamic analysis of the recombinant wild-type and of some site-directed mutants has revealed that the amino acid residues in the vicinity of CFMN play a very important role in governing the redox potential of CFMN and FeS. As a result, the semiquinone formation constant (K_S) of CFMN and the electron distribution constant (K_2) between CFMN and FeS are strongly influenced by the amino acid residues (*4*).

On the other hand, HmDH shows high substrate specificity towards histamine. Secondary and tertiary amines including biogenic amines such as tyramine do not react with the enzymes (*5*). Therefore, HmDH can be utilized in histamine analysis in food and clinical analysis (*6*, *7*). However, the one drawback is that the enzyme is strongly susceptible to the substrate inhibition from histamine at high concentrations (*2*, *4*). The substrate inhibition is considered to be a special case of the uncompetitive inhibition. Some interaction must exist between the substrate and the substrate-reduced enzyme (*4*). It has been reported that the equilibrium between the $CFMN_S$–FeS_R state and the $CFMN_R$–FeS_O state in the two-electron reduced subunit lies to the $CFMN_S$–FeS_R state at high concentrations of histamine. This seems to strongly be related to the substrate inhibition (*3*, *4*). Most probably, the second binding of histamine to $CFMN_S$ causes an increase in K_S of CFMN and the positive shift of the redox potential of the $CFMN_O/CFMN_S$ couple. The resulting up-hill electron transfer from $CFMN_S$ to FeS_O is responsible for the substrate inhibition (*4*). However, there is no report on the kinetic analysis of this process.

TMADH reaction with its physiological substrate, trimethylamine, has been studied by stopped flow spectroscopy and steady-state kinetics, with attention focusing on the substrate inhibition (*8*, *9*). Falzon *et al*. (*8*) reported that the CFMN cofactor is initially reduced by the substrate and one electron is then transferred intramolecularly from $CFMN_R$ to FeS_O. The latter reaction is reported to be biphasic. They proposed a model for the reductive half reaction of TMADH in which two molecules of the substrate bind to TMADH. One binds at the active site of the oxidized TMADH and is converted to the products. The other molecule binds but is not converted to product and influences the rate of the intramolecular electron transfer. Their steady-state and transient kinetic data are interpreted in the context of the crystal structure of TMADH (*8*). It is reported that the transient kinetics of TMADH with not only trimethylamine (*9*) but also diethylmethylamine (*10*) and dimethylbutylamine (*11*). They also proposed that the second binding of the substrate related to the substrate inhibition of TMADH, and that the plausible alternative redox cycles is responsible for the inhibition of the activity observed in the high-substrate regime. They demonstrated that the partitioning between the proposed two redox cycles depends on both trimethylamine and artificial electron acceptor concentration (*11*).

In this study, the stopped flow experiments of HmDH with histamine were performed on the basis of the spectral assignment of HmDH reported in a previous paper (*3*), in order to get our further understanding on the intramolecular and intersubunit electron transfer processes. The pH values were set at 7.5 and 10 for the experiments, since the switching of the redox property occurs at around pH 9 (*3*). In addition, the transient kinetic analysis was done to follow the substrate inhibition process. We also discuss a factor which causes the switching of the redox property at around pH 9.

Experimental Procedures

Enzyme purification

Recombinant wild-type HmDH was expressed in *E. coli* strain Rosetta (DE3) and purified as described previously (*12*). The protein concentration was determined using a modified Lowry method with DC Protein Assay Kit (Bio-Rad, USA) with bovine serum albumin as the standard protein. All chemicals used in this study were of analytical reagent grade and all solutions were prepared with distilled water.

Stopped flow spectrophotometry

Stopped-flow experiments were performed on an Applied Photophysics SX.18MV-R stopped flow spectrophotometer. The enzyme solution was then diluted with buffer (0.1 M potassium phosphate buffer for pH 7.5 and 0.1 M borate buffer for pH 10.0) to give a final concentration of 14 (365 and 440 nm), 28 (510 nm at pH 7.5) or 56 (510 nm at pH 10) μM, because of low molecular extinction coefficient at 510 nm. Histamine dihydrochloride used as the substrate was purchased from Sigma, and its solutions were prepared with the same buffer. Experiments were performed at 10°C by mixing HmDH in buffer of the desired pH, with an equal volume of histamine at desired concentration in the same buffer. For each substrate concentration used, at least four replicate measurements were corrected and averaged. HmDH does not use molecular oxygen as an electron transfer (*2*, *13*) and consequently these stopped flow experiments were carried out under aerobic conditions.

UV–vis spectroscopy

Steady-state kinetic measurements were performed with a quartz cuvette of a 1-cm light path at a final volume of 3 ml under anaerobic conditions at 30°C using a water jacket cell holder and a thermostat. Ferrocenium hexafluorophosphate (Fc^+) was obtained from Aldrich and used as an artificial electron acceptor, because its redox potential is sufficiently positive than that of the enzyme. Each of stock solutions of substrate and Fc^+ was added to the assay mixture to reach desired concentrations. Assays for the determination of kinetic parameters were performed in a 0.1 M potassium phosphate buffer of pH 7.5 and a 0.1 M borate buffer of pH 10. The reactions were initiated by the addition of the enzymes and the decrease in the absorbance at 617 nm due to the reduction of Fc^+ was measured using a Shimadzu UV-2500PC UV–vis recording spectrophotometer (Japan) (*14*).

UV–vis spectra of HmDH were obtained as described above earlier at a final volume of 2.5 ml. The HmDH solutions were prepared at concentrations of 3.1–4.2 μM in a 0.1 M potassium phosphate buffer of pH 7.5 and a 0.1 M borate buffer of pH 10.

Results

Steady-state kinetics of HmDH with histamine

The steady-state kinetics of HmDH with histamine has been studied at pH 7.5 and 10 and at 30°C. The dependence of the initial velocity (v) on the histamine concentration over the range from 10 μM to 1 mM is

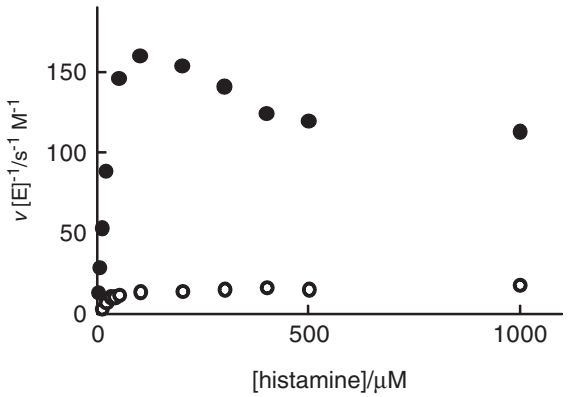

Fig. 1 Steady-state kinetic analysis of the reaction of HmDH at pH 7.5 and 10. Closed circles, data for pH 7.5 are taken from previously published results (*4*); open circles, data for pH 10. Note that the experiments with histamine performed at 30°C.

shown in Fig. 1. The substrate inhibition is observed at the histamine concentration over 100 μM at pH 7.5. On the other hand, at pH 10 the enzyme kinetics exhibited a standard Michelis–Menten-like dependence on the histamine concentration. The $v\ [E]^{-1}$ value at pH 10 is only 16% of that at pH 7.5 at the histamine concentration of 1 mM.

Reductive half-reaction kinetics at pH 7.5

$CFMN_O$ shows a strong and characteristic absorption band at 440 nm, while $CFMN_S$ shows two sharp absorption bands at 365 and 440 nm and a broad band at around 510 nm (*3*). $CFMN_R$ does not have any characteristic absorption band at the wavelength over 350 nm (*3*). The absorption band of FeS_O is not clearly resolved, but must have a broad tail at the wavelength less than 500 nm, as guessed from the absorption property of some bacterial-type ferredoxins (*15–17*). The tailed absorption decreases on the reduction of the cluster (*15–17*). Considering these absorption characteristics of the two redox centers in HmDH, stopped flow spectrophotometry was performed at 365, 440 and 510 nm for the reductive half reaction of HmDH at various concentrations of histamine. Data points were collected for each kinetic transient. The absorbance change associated with the fast phase of the reaction was corrected for the dead time of the stopped flow apparatus (~1.4 ms). A set of stopped flow spectrophotometric data is given in Fig. 2. The fast decrease in the absorbance at 440 nm (Fig. 2B) is predominantly ascribed to a fast decrease in $CFMN_O$ (flavin bleaching). The sharp decrease in the absorbance at 510 nm in the beginning of the reaction is also caused by the fast decrease in $CFMN_O$ (Fig. 2C). The subsequent slow increase in the absorbance is due to the generation of $CFMN_S$ caused by a single electron transfer from $CFMN_R$ to FeS_O. Such increase in $CFMN_S$ is also evidenced from the absorbance change at 365 nm (Fig. 2A).

Therefore, we first tried to analyse a set of the data on a kinetic model with two sequential first-order reaction phases. The concentration of histamine used was always at least 10-fold greater than that of HmDH, thereby ensuring pseudo-first-order

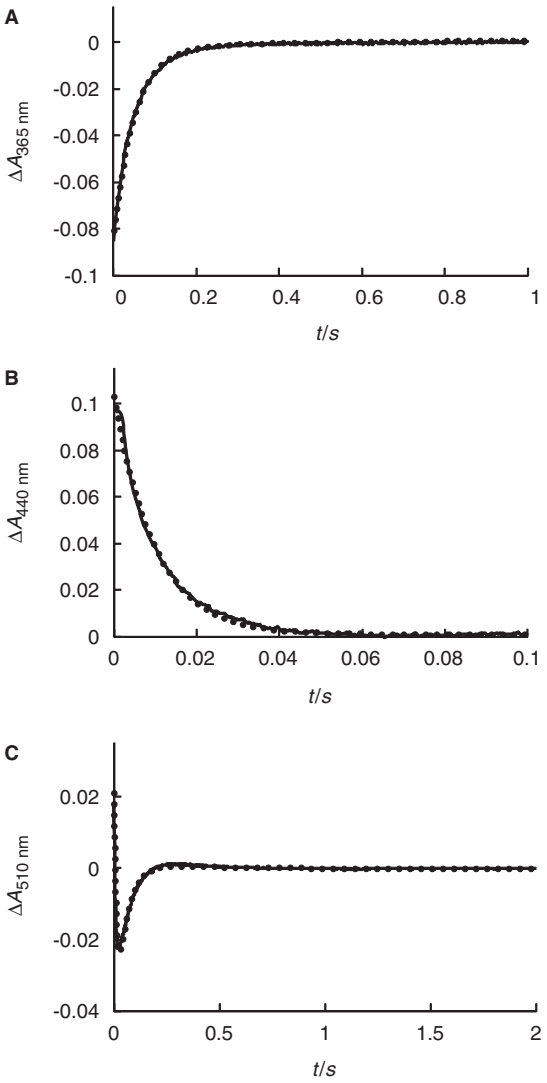

Fig. 2 Kinetic transients for the reaction of oxidized HmDH with histamine at pH 7.5. Absorbance changes observed at (A) 365 nm, (B) 440 nm and (C) 510 nm. Reaction conditions after mixing were: 14 μM (365 nm and 440 nm) and 28 μM (510 nm) HmDH, 800 μM histamine, 0.1 M potassium phosphate buffer, pH 7.5, 10°C. The dotted lines represent the data points and the solid lines represent the best fits of the data based on equation (*1*). Rate constants obtained from fit are: $k_a = 74\ s^{-1}$, $k_b = 17\ s^{-1}$ and $k_c = 1.7\ s^{-1}$.

conditions in any substrate-dependent process. However, clear reproduction was not obtained by a non-linear least square fitting of a corresponding equation to a set of the data. We considered that the reason is due to the fact that the concentration of histamine used was in the region to cause the substrate inhibition, during which the $CFMN_S$ concentration increases somewhat (*4*). Therefore, we tried to analyse sets of the data on a kinetic model with three sequential first-order reaction phases. The overall kinetic is consistent with a following reaction mechanism:

$$E_{Ox} + S \xrightarrow{k_a} I \xrightarrow{k_b} II \xrightarrow{k_c} III$$

Scheme 1

where E_{ox} represents the oxidized HmDH containing $CFMN_O$ and FeS_O, S represents substrate (*4*) and I, II

and III represent discrete intermediate species which are generated in the fast, moderate and slow kinetic phases, respectively. The kinetic equation is given by

$$\Delta A = \Delta A_a \exp(-k_a t) + \Delta A_b \exp(-k_b t) + \Delta A_c \exp(-k_c t) \quad (1)$$

where ΔA is the total absorbance change at a given wavelength and at a given time (t). The rate constants of the fast, moderate and slow processes are given by k_a, k_b and k_c, respectively ($k_a >> k_b >> k_c$) and ΔA_a, ΔA_b and ΔA_c are related to the absorbance change due to the fast, moderate and slow phases, respectively, at a given wavelength. The experimental data were well reproduced by a non-linear least square analysis using equation (*1*) as shown in Fig. 2, where the fitting parameters used are three rate constants k_a, k_b and k_c and three sets of ΔA_a, ΔA_b and ΔA_c at each wavelength. The refined rate constants k_a, k_b and k_c are plotted against the histamine concentration in Fig. 3. The series of the refined rate constants seem to satisfy the assumption used in the analysis that $k_a >> k_b >> k_c$.

The first fast phase can be assigned to a direct two-electron reduction of $CFMN_O$ by histamine with no involvement of $CFMN_S$, because the $CFMN_S$ generation as observed at 365 nm is much slower than the $CFMN_O$ decrease (bleaching) as observed at 510 and 440 nm (in the time range <0.02 s). The rate constant of the fast phase k_a exhibited a hyperbolic dependence on the concentration of histamine (Fig. 3A). Similar phenomena have been reported for TMADH (*8*, *9*). Therefore, Species I in Scheme 1 should represent the two-electron-reduced enzyme containing $CFMN_R$ and FeS_O. The fast phase consists of the formation of a Michaelis complex between HmDH and histamine and the subsequent bleaching of the flavin, as shown in Scheme 2.

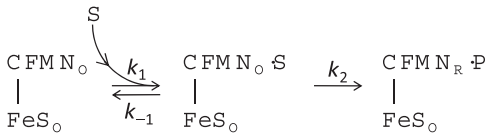

Scheme 2

where k_1, k_{-1} and k_2 are the rate constants of the corresponding processes and P is the product. Assumption of a rapid equilibrium in the enzyme-substrate complex formation ($k_2 << k_{-1}$) leads to equation (*2*):

$$k_a = \frac{k_2[S]}{K_{d1} + [S]}, \quad (2)$$

where [S] is the substrate concentration and K_{d1} is the apparent dissociation constant of the enzyme-substrate complex formation ($K_{d1} = k_{-1}/k_1$). Equation (*2*) was fit to the data to obtain the rate constants of $k_2 = 1.3 \times 10^2\,s^{-1}$ and $K_{d1} = 1.4 \times 10^2\,\mu M$.

The rate constant of the moderate phase (k_b) was almost independent of the substrate concentration (Fig. 3B). Thus, the process can be reasonably assigned to an intramolecular electron transfer. As described

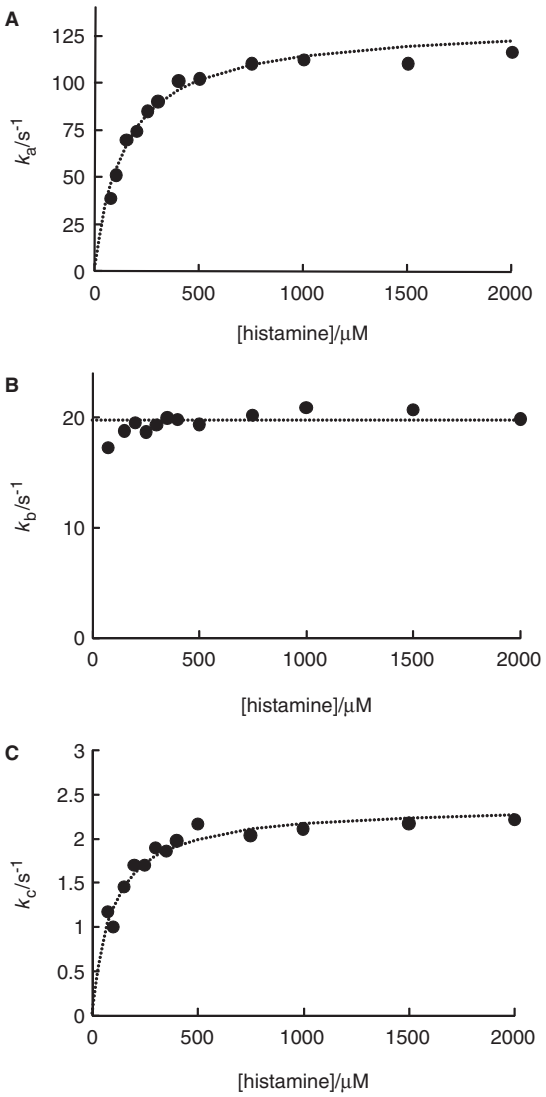

Fig. 3 Dependence of (A) ka, (B) kb and (C) kc on the substrate concentration at pH 7.5. Closed circles represent values of rate constants obtained from fits of kinetic transients. The dotted lines represent the corresponding regression curves (see the text for detail).

earlier, the characteristic increase in the absorbance at 510 nm following the fast decrease seems to strongly reflect the single-electron transfer step from $CFMN_R$ to FeS_O to generate $CFMN_S$ to FeS_R (Scheme 3), and then we can conclude that $k_b = k_3$.

The k_3 value was averaged to be $2.0 \times 10\,s^{-1}$ in the histamine concentration range from 0.2 to 2 mM.

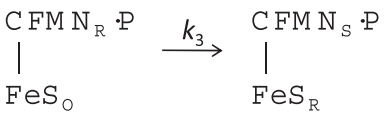

Scheme 3

In the third slow phase, the small absorbance increase occurred at 365 nm ($\Delta A_b >> \Delta A_c$). Such absorption change is observed at high concentrations of histamine in the substrate titration. The slow phase is a pseudo-first order reaction and the rate constant (k_c) exhibited a hyperbolic dependence on the histamine concentration (Fig. 3C). Thus, the process can be assigned to the second binding of histamine to the

$CFMN_S$–FeS_R state of the two-electron reduced HmDH, as shown by (Scheme 4)

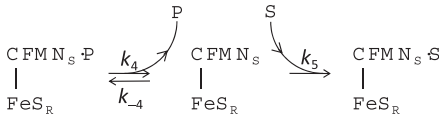

Scheme 4

Assuming a rapid equilibrium in the release of the product ($k_5 << k_{-4}$), the overall rate constant of the slow process is given by

$$k_c = \frac{k_5[S]}{K_{d2} + [S]} \quad (3)$$

where K_{d2} is the apparent dissociation constant of the product enzyme complex ($K_{d2} = k_4/k_{-4}$). In the dynamic enzyme reaction (that is, for example, the reaction under steady-state conditions), the reverse reaction of the second substrate binding must be considered. However, for simplification, we assumed an irreversible process, since we are focusing on the reductive half reaction in the presence of excess amount of the substrate. The best fit of equation (*3*) to the data in Fig. 3C yielded that $k_5 = 2.4\,s^{-1}$ and $K_{d2} = 9.7 \times 10\,\mu M$.

On the other hand, it is noteworthy that K_{d2} is smaller than K_{d1}. This means that the product binding reaction is favoured compared with the substrate binding reaction. This situation may lead product inhibition, which might be responsible in part to the substrate inhibition phenomena in the steady-state kinetics. However, there is a clear spectroscopic evidence of the interaction between the substrate-reduced enzyme and the substrate (*4*). Therefore, we believe that the second binding of the substrate is responsible for the substrate inhibition.

Reductive half-reaction kinetics at pH 10

In contrast to the case at pH 7.5, the monotonous decrease in the absorbance was observed at pH 10 without an increasing phase at 510 nm (Fig. 4C) as well as at 365 and 440 nm (Fig. 4A and B, respectively), suggesting a fast disappearance of the $CFMN_R$ intermediate generated in the first step of the substrate reduction. The absorption transient was well analysed on a model with single kinetic phase at 365, 440 and 510 nm, as shown in Fig. 4. The kinetics is expressed by

$$\Delta A = \Delta A_d \exp(-k_d t). \quad (4)$$

The pseudo-first-order rate constant (k_d) exhibited a hyperbolic dependence on the histamine concentration (Fig. 5). Under the conditions, the one-electron reduction occurs per subunit in the substrate reduction to generate the $CFMN_S$–FeS_O form, most probably by an intersubunit single-electron transfer from $CFMN_R$

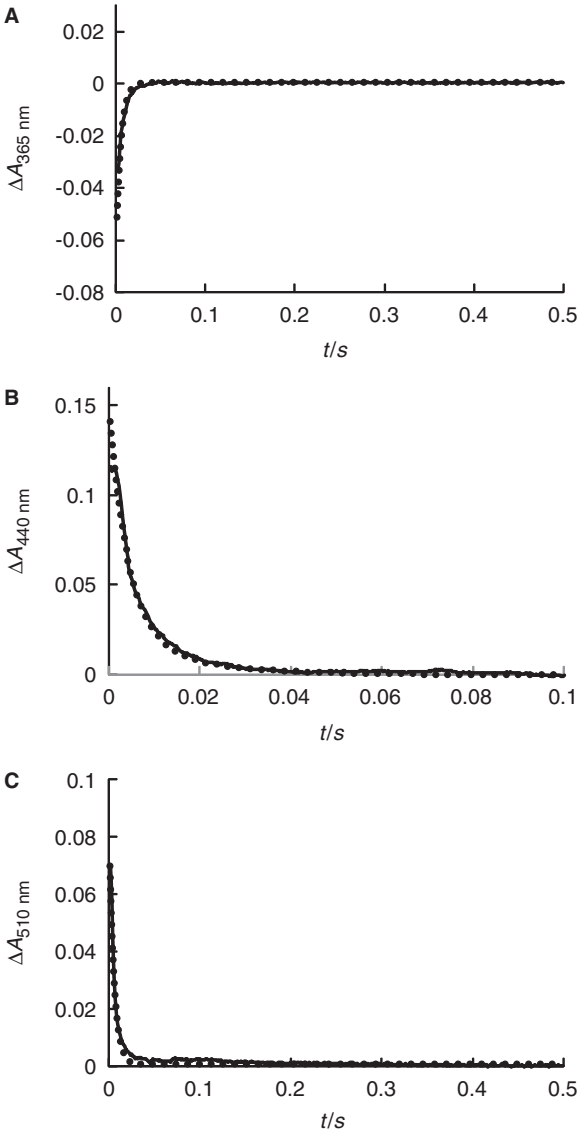

Fig. 4 Kinetic transients for the reaction of the oxidized HmDH with histamine at pH 10. Absorbance changes observed at (A) 365 nm, (B) 440 nm and (C) 510 nm. Reaction conditions after mixing were: 14 μM (365 and 440 nm) and 56 μM (510 nm) HmDH, 800 μM histamine, 0.1 M borate buffer, pH 10, 10°C. The dotted lines represent the data points and the solid lines represent fits of the data based on equation (*4*). Rate constants obtained from fit are $k_d = 1.9 \times 10^2\,s^{-1}$.

of one subunit to $CFMN_O$ of the other subunit (*3*). As a result, we can conclude that the rate of the intersubunit electron transfer is much faster than that of the first two-electron reduction of $CFMN_O$ of one subunit by histamine. The reaction mechanism for the (apparently) single kinetic phase is given as shown in Scheme 5, although we do not have clear evidence of the product release.

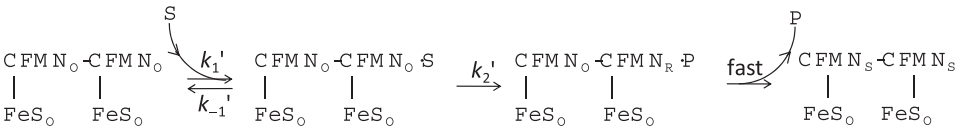

Scheme 5

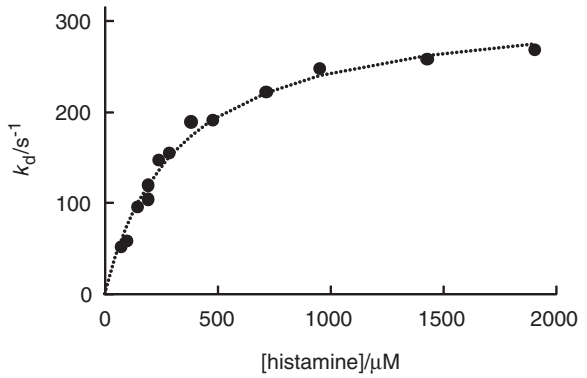

Fig. 5 Dependence of k_d on the substrate concentration at pH 10. Closed circles represent values of rate constants obtained from fits of kinetic transients. The dotted line represents the regression curves based on equation (*5*).

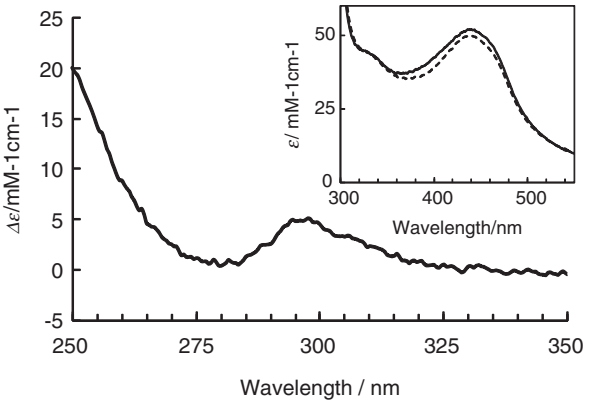

Fig. 6 UV-difference spectrum obtained by subtracting the spectrum of HmDH at pH 10 from that at pH 7.5. The inset shows the UV–vis spectra of oxidized HmDH at pH 7.5 (solid line) and 10 (dashed line) in 0.1 M potassium phosphate and 0.1 M borate buffer, respectively.

The rapid equilibrium assumption in the Michaelis complex formation leads to the relation:

$$k_d = \frac{k'_2[S]}{K'_{d1} + [S]} \quad \left(k'_{d1} = k'_{-1}/k'_1\right). \tag{5}$$

The best fit of the concentration dependence of the refined k_d yielded that $k_2' = 3.2 \times 10^2\,s^{-1}$ and $K_{d1}' = 6.8 \times 10^2\,\mu M$.

UV–vis spectroscopy of HmDH

In order to find a factor which causes the switching in the reductive half-reaction property at around pH 9, we measured UV–vis spectra of HmDH. Small but clear difference in the absorption spectrum is observed between at pH 7.5 and 10 (Fig. 6, inset). The UV-difference spectrum was obtained by subtracting the spectrum of HmDH at pH 10 from that at pH 7.5, and the difference spectrum gives a peak at around 295 nm (Fig. 6). The spectral change due to the deprotonation of the flavin itself is expected to be much larger (*18*), and then the change in the absorption can be assigned to the deprotonation of Tyr residue(s) in the oxidized form of HmDH. Trp might be also a candidate but should be ruled out, because the spectral change of Trp is very small on the deprotonation (Supplementary Fig. S1B) in contrast to Tyr, which shows a large spectral change centered at around 295 nm (Supplementary Fig. S1A). The conclusion is also supported by fluorescence spectral measurements. The protein fluorescence emission ($\lambda_{ex} = 295$ nm) is usually dominated by the Trp fluorescence. However, the fluorescence spectra ($\lambda_{ex} = 295$ nm) of HmDH at pH 7.5 and 10 are almost identical with each other (data not shown). Number of the Tyr residue dissociated may be evaluated as about 2 from the spectral change (an absorption coefficient difference of Tyr is $2.5\,mmol^{-1}\,cm^{-1}$ and that of HmDH is $4.8\,mmol^{-1}\,cm^{-1}$).

Discussion

The reductive half reaction of HmDH with histamine can be successfully interpreted on a three sequential first-order reaction phase model (Scheme 1) at pH 7.5, where the two-electron reduction occurs in each subunit and HmDH is strongly susceptible to the substrate inhibition for histamine (*4*). The first fast step is the flavin bleaching (i.e. the direct two-electron reduction of $CFMN_O$ by histamine) via a Michaelis complex to generate $CFMN_R$ (Scheme 2). The subsequent moderate process is the intramolecular single-electron transfer from $CFMN_R$ to FeS_O (Scheme 3), of which the kinetics is independent of the substrate concentration (Fig. 3B). The final slow process is the second substrate binding responsible for the substrate inhibition (Scheme 4). The proposed analytical model is very useful in the study of the intramolecular single-electron transfer from $CFMN_R$ to FeS_O, because the extraction of intramolecular kinetic information is very difficult. This third slow process is accompanied by small increase of $CFMN_S$ in our stopped flow experiments. The hyperbolic dependence of the rate constant on the histamine concentration (Fig. 3C) strongly suggests the second binding of the substrate to the substrate-reduced enzyme.

We have already evaluated the redox potential of the CFMN and [4Fe–4S] cluster in the enzyme (*3*) and shown that the substrate-derived two-electron-reduced form has two ultimate states; $CFMN_S$–$CFMN_R$ and $CFMN_R$–FeS_O.

$$CFMN_O + e^- \rightleftarrows CFMN_S \qquad E^{\circ\prime}_{O/S} \tag{6a}$$

$$CFMN_S + e^- \rightleftarrows CFMN_R \qquad E^{\circ\prime}_{S/R} \tag{6b}$$

$$FeS_O + e^- \rightleftarrows FeS_R \qquad E^{\circ\prime}_{FeS} \tag{6c}$$

The distribution equilibrium between two states is a function of $E^{\circ\prime}_{S/R}$ and $E^{\circ\prime}_{FeS}$:

$$K_2 \equiv \frac{[CFMN_S\text{–}FeS_R]}{[CFMN_R\text{–}FeS_O]} = \exp(F(E^{\circ\prime}_{FeS} - E^{\circ\prime}_{S/R})/RT) \tag{7}$$

where F, R and T are the Faraday constant, the gas constant and the absolute temperature, respectively. The second binding of histamine to the

substrate-reduced enzyme perturbs the redox potential to increase the K_2 value (*4*). The increase in K_2 is accompanied by an increase in the semiquinone formation constant (or comproportionation constant, K_S) (*4*), which is defined by

$$K_S = \frac{[CFMN_S]^2}{[CFMN_O][CFMN_R]} = \exp(F(E^{\circ\prime}_{O/S} - E^{\circ\prime}_{S/R})/RT) \quad (8)$$

Under the conditions, $E^{\circ\prime}_{O/S}$ tends to be more positive than $E^{\circ\prime}_{FeS}$. Therefore, the second step of the two sequential single electron transfers from the reduced flavin to the [4Fe–4S] cluster is not favoured. We believe that this is the scenario of the substrate inhibition.

At pH 10, where single-electron reduction per monomer occurs (*3*) and HmDH does not suffer from the substrate inhibition (*4*). The overall kinetics is described on a single pseudo-first order phase to yield the $CFMN_S$–FeS_O state. Under such conditions, one of the subunits must first be reduced by one molecule of histamine to generate a heterogeneous redox state dimer consisting of the $CFMN_R$–FeS_O subunit and the $CFMN_O$–FeS_O subunit. Subsequently, a single-electron transfer occurs from the $CFMN_R$–FeS_O subunit to the $CFMN_O$–FeS_O subunit to generate a homogeneous dimer composed of the $CFMN_S$–FeS_O subunits (Scheme 3). The thermodynamic driving force of the single electron transfer is guaranteed by a large K_S value at pH 10 ($K_S = 1.9 \times 10^2$), which is compared that at pH 7.5 ($K_S = 1.8$) (*3*, *4*). From the thermodynamic viewpoint, a comproportional intermolecular single-electron transfer from a partially reduced heterogeneous enzyme with $CFMN_R$–FeS_O and CFMNo–FeS_O to the fully oxidized enzyme to generate other partially reduced homogeneous enzyme with FMN_S–FeS_O. However, the process has been ruled out in the previous paper (*3*), and if any, the rate will be very slow in such diluted enzyme solution. Thus, we will focus on the intrersubunit electron transfer in the molecule from the $CFMN_R$–FeS_O subunit to the $CFMN_O$–FeS_O subunit.

Interestingly, the k_2' value (at pH 10) is about three times as large as k_2 (at pH 7.5). This might be due to the increase in the basicity of the substrate at increased pH. However, $v\,[E]^{-1}$ at pH 10 obtained in the steady-state kinetics is only 16% of that at pH 7.5 (Fig. 1). This means that the electron transfer from the substrate to the enzyme is not the rate determining step in the steady-state kinetics experiments at pH 10. The mechanism in Scheme 5 suggests very small K_2 as well as very large K_S. Under the condition of very small K_2, the first single electron transfer from $CFMN_R$ to FeS_O should be thermodynamically unfavourable, and seems to behave as a rate determining step. The situation decreases the steady-state enzyme reaction rate.

On the other hand, we cannot clarify whether the second substrate binding of occurs at pH 10. This is also due to large K_S, because extremely large potential perturbation is required for further increase in K_S. As a result, the enzyme does not suffer from the substrate inhibition at pH 10. This kind of the reaction property is observed in histamine dehydrogenase from *Rhizobium* sp. 4–9, which does not suffer from the substrate inhibition even at neutral pH although the catalytic constant is small (*4*, *19*).

Here, we also attempted to consider a factor to cause the intrersubunit electron transfer from the $CFMN_R$–FeS_O subunit to the $CFMN_O$–FeS_O subunit at pH 10. Comparison of the UV–vis spectra of HmDH at pH 7.5 and 10 suggests the deprotonation of Tyr residues in HmDH. Tyr residues often play very important roles in relaying electrons in proteins (*20*, *21*). Many studies have addressed electron transfer reactions which proceeds almost passively in the protein matrix from electron donor to acceptor (*22*–*25*). For the high redox potentials of the electron acceptors in some electron transfer proteins, Tyr residues, can potentially and actively participate in the electron transfer, becoming alternatively oxidized and reduced as semiconductor relay elements. In our previous report, we have shown that $E^{\circ\prime}_{FeS}$ shifts in the direction of the negative potential with pH at pH >9 (*3*). This may be due to the deprotonation of Tyr residures near FeS in HmDH, as is suggested in *E. coli* dimethylsulfoxide reductase, where a Tyr residue plays a major role in controlling the redox properties of an iron–sulphur cluster and for communication between an iron–sulphur cluster and the quinol-binding site (*26*). Thus, the deprotonation of Tyr residues near CFMN and FeS at pH 10 seems to perturb the redox potential to decrease K_2 as well as increase K_S and simultaneously to facilitate the intersubunit electron transfer in HmDH.

In conclusion, the present work has revealed the intramolecular electron transfer process of HmDH at pH 7.5 and 10. The kinetic profile obtained by the stopped flow experiments is in accord with the thermodynamic properties. The deprotonation of Tyr residues near CFMN and FeS in HmDH seems to cause the switching in the electron transfer property.

Supplementary Data

Supplementary Data are available at *JB* Online.

Acknowledgements

We thank Dr Nobutaka Fujieda and Ms Hanae Suzuki for the assistant to the stopped flow experiments.

Funding

This work was supported in part by Grants-in-Aids for Scientific Research from the Ministry of Education, Science, Sports and Culture of Japan (to M. T. 20.3618 and to K. K. 15380082 and 19310070).

Conflict of interest

None declared.

References

1. Fujieda, N., Satoh, A., Tsuse, N., Kano, K., and Ikeda, T. (2004) 6-*S*-Cysteinyl flavin mononucleotide-

containing histamine dehydrogenase from *Nocardioides simplex*: molecular cloning, sequencing, overexpression, and characterization of redox centers of enzyme. *Biochemistry* **43**, 10800–10808
2. Limburg, J., Mure, M., and Klinman, J. P. (2005) Cloning and characterization of histamine dehydrogenase from *Nocardioides simplex*. *Arch. Biochem. Biophys.* **436**, 8–22
3. Tsutsumi, M., Fujieda, N., Tsujimura, S., Shirai, S., and Kano, K. (2008) Thermodynamic redox properties governing half-reduction characteristics of histamine dehydrogenase from *Nocardioides simplex*. *Biosci. Biotechnol. Biochem.* **72**, 786–796
4. Tsutsumi, M., Fujieda, N., Tsujimura, S., Shirai, S., and Kano, K. (2010) Site-directed mutation at residues near the catalytic site of histamine dehydrogenase from *Nocardioides simplex* and its effects on substrate inhibition. *J. Biochem.* **147**, 257–264
5. Siddiqui, J.A., Shoeb, S.M., Takayama, S., Shimizu, E., and Yorifuji, T. (2000) Histamine dehydrogenase of *Nocardioides simplex*: a second bacterial enzyme for histamine degradiation. *J. Biochem. Mol. Bio. Biophys.* **5**, 37–43
6. Takagi, K. and Shikata, S. (2004) Flow injection determination of histamine with a histamine dehydrogenase-based electrode. *Anal. Chim. Acta* **505**, 189–193
7. Yamada, R., Fujieda, N., Tsutsumi, M., Tsujimura, S., Shirai, O., and Kano, K. (2008) Bioelectrochemical determination at histamine dehydrogenase-based electrodes. *Electrochemistry* **76**, 600–602
8. Falzon, L. and Davidson, V.L. (1996) Kinetic model for regulation by substrate of intramolecular electron transfer in trimethylamine dehydrogenase. *Biochemistry* **35**, 2445–2452
9. Jang, M.-H., Basran, J., Scrutton, N.S., and Hille, R. (1999) The reaction of trimethylamine dehydrogenase with trimethylamine. *J. Biol. Chem.* **274**, 13147–13154
10. Rohlfs, R.J. and Hille, R. (1994) The reaction of trimethylamine dehydrogenase with diethylmethylamine. *J. Biol. Chem.* **269**, 30869–30879
11. Roberts, P., Basran, J., Wilson, E.K., Hille, R., and Scrutton, N.S. (1999) Redox cycles in trimethylamine dehydrogenase and mechanism of substrate inhibition. *Biochemistry* **38**, 14927–14940
12. Fujieda, N., Tsuse, N., Satoh, A., Ikeda, T., and Kano, K. (2005) Production of completely flavinylated histamine dehydrogenase, unique covalently bound flavin, and iron-sulfur cluster-containing enzyme of *Nocardioides simplex* in *Escherichia coli*, and its properties. *Biosci. Biotechnol. Biochem.* **69**, 2459–2462
13. Suddiqui, J.A., Shoeb, S.M., Takayama, S., Shimizu, E., and Yorifuji, T. (2000) Purification and characterization of histamine dehydrogenase from *Nocardioides simplex* IFO 12069. *FEMS Microbiol. Lett.* **189**, 183–187
14. Wilson, E.K., Mathews, F.S., Packman, L.C., and Scrutton, N.S. (1995) Electron tunneling in substrate-reduced trimethylamine dehydrogenase: kinetics of electron transfer and analysis of the tunneling pathway. *Biochemistry* **34**, 2584–2591
15. Stombaugh, N.A., Sundquist, J.E., Burris, R.H., and Orme-Johnson, W.H. (1976) Oxidation-reduction properties of several low potential iron-sulfur proteins and of methylvolgen. *Biochemistry* **15**, 2633–2641
16. Chen, K., Bonagura, C.A., Tilley, G.J., McEvoy, J.P., Jung, Y.-S., Armstrong, F.A., Stout, C.D., and Burgess, B.K. (2002) Crystal structures of ferredoxin variants exhibiting large changes in [Fe-S] reduction potential. *Nat. Struct. Biol.* **9**, 188–192
17. Teixeira, M., Batista, R., Campos, A.P., Gomes, C., Mendes, C., Pacheco, I., Anemuller, S., and Hagen, W.R. (1995) A seven-iron ferredoxin from the thermoacidophilic archaeon *Desulfurolobus ambivalens*. *Eur. J. Biochem.* **227**, 322–327
18. Massey, V. and Hemmerich, P. (1980) Active-site probes of flavoproteins. *Biochem. Rev.* **8**, 246–257
19. Bakke, M., Sato, T., Ichikawa, K., and Nishimura, I. (2005) Histamine dehysrogenase from *Rhizobium* sp.: Gene cloning, expression in *Escherichia coli*, characterization and application to histamine determination. *J. Biotechnology* **119**, 260–271
20. Miles, C.S., Rouvière-Formy, N., Lederer, F., Mathews, F.S., Reid, G.A., Black, M.T., and Chapmen, S.K. (1992) Tyr-143 facilitates interdomain electron transfer in flavocytochrome b_2. *Biochem. J.* **285**, 187–192
21. Rouvière, N., Mayer, M., Tegoni, M., Capeillère-Blandin, C., and Lederer, F. (1997) Molecular interpretation of inhibition by excess substrate in flavocytocherome b_2: A study with wild-type and Y143F mutant enzymes. *Biochemistry* **36**, 7126–7135
22. Onuchic, J.N., Beratan, D.N., Winkler, J.R., and Gray, H.B. (1992) Pathway analysis of protein electron-transfer reactions. *Annu. Rev. Biophys. Biomol. Struct.* **21**, 349–377
23. Wuttke, D.S., Bjerrum, M.J., Winkler, J.R., and Gray, H.B. (1992) Electron-tunneling pathways in cytocherome *c*. *Science* **256**, 1007–1009
24. Bollinger, J.M. (2008) Electron relay in Proteins. *Science* **320**, 1730–1731
25. Shih, C., Museth, A.K., Abrahamsson, M., Blanco-Rodriduez, A.M., Di Bilio, A.J., Sudhamsu, J., Crane, B.R., Ronayne, K.L., Towrite, M., Vlček, A., Richards, J.H., Winkler, J.R., and Gray, H.B. (2008) Tryptophan-accelerated electron flow through proteins. *Science* **320**, 1760–1762
26. Cheng, V.W.T., Rothery, R.A., Bertero, M.G., Strynadka, N. C.J., and Weiner, J.H. (2005) Investigation of the environment surrounding iron-sulfur cluster 4 of *Escherichia coli* dimethylsulfoxide reductase. *Biochemistry* **44**, 8068